EPJ Web of Conferences **120**, 01001 (2016) DOI: 10.1051/epjconf/201612001001
ISMD 2015

Bose-Einstein correlations and results on minimum bias interactions, underlying event and particle production from ATLAS

Yuri Kulchitsky[1,2,a] (on behalf of the ATLAS Collaboration)

[1] *Institute of Physics, National Academy of Sciences, Minsk, Belarus*
[2] *JINR, Dubna, Russia*

Abstract. The report on the recent results of soft-QCD with the ATLAS experiment at the LHC is presented. The effect of space-time geometry in the hadronization phase has been studied in the context of Bose-Einstein correlations between charged particles, for determining the size and shape of the source from which particles are emitted. Bose-Einstein correlation parameters are investigated in proton-proton collisions at 0.9 and 7 TeV, up to very high charged particle multiplicities. Measurements of the properties of charged particle production are presented from proton-proton collisions at different centre-of-mass energies in the range of 0.9 to 13 TeV and compared to various Monte Carlo event generator models. Furthermore, particle distributions sensitive to the underlying event have been measured and are compared to theoretical models. The production properties of mesons and baryons are presented and compared to predictions.

1 Introduction

The focus of the ATLAS experiment [1] at the LHC is high-p_{T} physics, and also provides a window into important softer QCD processes. These are of intrinsic interest but also their understanding underpins searches for new physics. The selected topics of this paper, including first 13 TeV results, are Bose Einstein correlations [2], charged particledistributions [3], underlying events for leading tracks at 13 TeV [4], Z-boson [5] and jets [6] at 7 TeV, and particleproduction [7, 8] at 7 TeV. The ATLAS Collaboration possess now data from 0.9 to 13 TeV in the same detector, allowing scale evolution to be probed.

2 Bose-Einstein correlations at 0.9 and 7 TeV

The studies of Bose–Einstein Correlations (BEC) for pairs of like-sign charged particles measured in the kinematic range $p_{\mathrm{T}} > 100$ MeV and $|\eta| < 2.5$ in proton–proton collisions at centre-of-mass energies of 0.9 and 7 TeV with the ATLAS detector are presented [2]. The integrated luminosities are approximately 7 $\mu\mathrm{b}^{-1}$, 190 $\mu\mathrm{b}^{-1}$ and 12.4 nb^{-1} for 0.9 TeV, 7 TeV minimum-bias (MB) and 7 TeV high-multiplicity (HM) data samples, respectively. Bose–Einstein correlations are measured in terms of a two-particle correlation function, $C_2(p_1, p_2) = \rho(p_1, p_2)/\rho_0(p_1, p_2) = C_0[1 + \lambda \cdot \exp(-RQ)](1 + \varepsilon Q)$, where p_1 and p_2 are the four-momenta of two identical bosons in the event, ρ is the two-particle density function, and ρ_0 is a two-particle density function (known as the reference function) specially

[a] e-mail: Iouri.Koultchitski@cern.ch

constructed to exclude BEC effects, $Q^2 = -(p_1 - p_2)^2$, and C_0, R, λ, ε are parameters. The unlike-charge reference sample is used. To account for the effects of resonances, the two-particle correlation function $C_2(Q)$ is corrected using Monte Carlo simulation without BEC effects via a double-ratio correlation function defined as $R_2(Q) = C_2(Q)/C_2^{MC}(Q)$. There are no the anti-correlations in the $R_2(Q)$ correlation functions. The multiplicity and k_T dependences are shown in the Fig. 1 for the R (top) and λ (bottom) parameters. The R parameter (Fig. 1 (a)) increases with multiplicity up to about $n_{ch} \simeq 50$ independently of the center of mass energy. For $n_{ch} \leq 82$ at 0.9 TeV and $n_{ch} \leq 55$ at 7 TeV, the n_{ch} dependence on R is fitted with the function $R(n_{ch}) = \alpha\sqrt[3]{n_{ch}}$. The n_{ch} dependence on R at 7 TeV is fitted for $n_{ch} > 55$ with a constant and $R(n_{ch}) = 2.28 \pm 0.32$ fm. A saturation effect in the multiplicity dependence of the correlation source size parameter is observed. The k_T dependence of the R parameter (Fig. 1 (b), (c)) is found to follow an exponential decrease. The shapes of the k_T dependence are similar for the 7 TeV and the 7 TeV HM data. The λ parameter exponentially decreases with multiplicity (Fig. 1 (d)) and k_T (Fig. 1 (e), (f)).

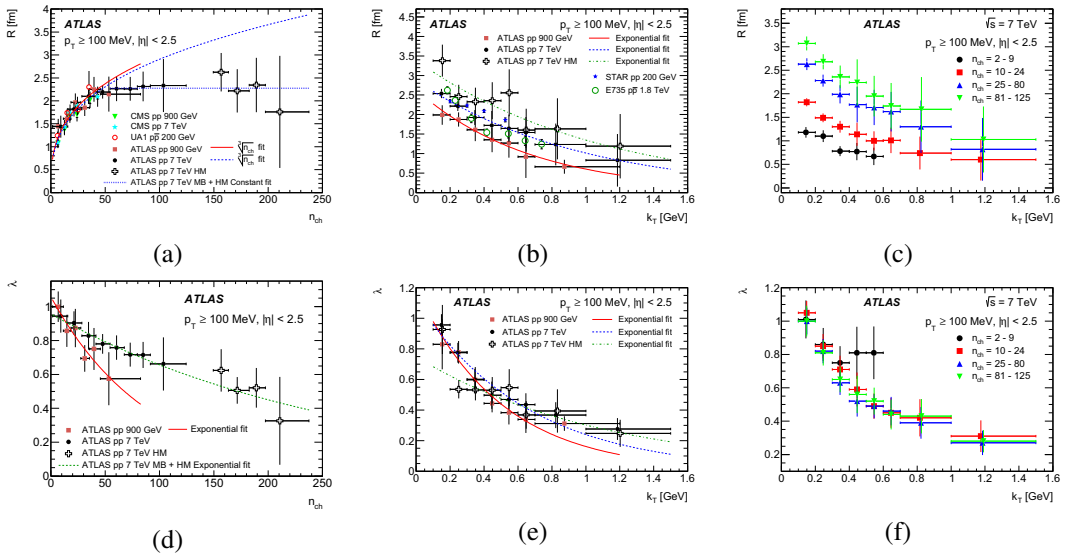

Figure 1. Dependences of the R (top) and λ (bottom) BEC parameters on (a, d) multiplicity, n_{ch}, and (b, e) pair transverse momentum, $k_T = |\mathbf{p}_{T,1} + \mathbf{p}_{T,2}|/2$, obtained from the exponential fit to the two-particle double-ratio correlation functions $R_2(Q)$ at 0.9 and 7 TeV and 7 TeV HM events (taken from Ref. [2]). The solid and dashed curves are the results of (d) the exponential and (a) $\sqrt[3]{n_{ch}}$ for $n_{ch} \leq 55$ fits. The dotted line in (a) is a result of a constant fit to MB and HM events data at 7 TeV for $n_{ch} > 55$. The solid, dashed and dash-dotted curves on (b) and (c) are results of the exponential fits for 0.9 TeV, 7 TeV and 7 TeV HM data, respectively. The results on the (b) are compared to the corresponding measurements by the E735 experiment at the Tevatron [9], and by the STAR experiment at RHIC [10]. The k_T dependence of the fitted parameters (c) R and (f) λ obtained from the exponential fit to the $R_2(Q)$ correlation function at 7 TeV for the different multiplicity regions: $2 \leq n_{ch} \leq 9$ (circles), $10 \leq n_{ch} \leq 24$ (squares), $25 \leq n_{ch} \leq 80$ (triangles) and $81 \leq n_{ch} \leq 125$ (inverted triangles).

3 Charged particle distributions at 13 TeV

Measurements of charged particle distributions in pp collisions at 13 TeV are presented, using a data sample of nearly 9 million events recorded by the ATLAS detector, corresponding to an integrated luminosity of $\approx 170\ \mu b^{-1}$ [3]. The corrected distributions for primary charged particles for events with $n_{ch} \geq 1$ in the kinematic range $p_T > 500$ MeV and $|\eta| < 2.5$ are shown in Fig. 2. In most bins of all distributions the largest uncertainty comes from the track reconstruction efficiency. Fig. 2 (a) shows

the charged particle multiplicity as a function of pseudorapidity. The mean particle density is roughly constant at 2.9 for $|\eta| < 1.0$ and decreases at higher values of $|\eta|$. Fig. 2 (b) shows the charged particle multiplicity as a function of transverse momentum. Fig. 2 (c) shows the charged particle multiplicity distribution. Fig. 2 (d) shows the mean transverse momentum versus the charged particle multiplicity. The $\langle p_{\mathrm{T}} \rangle$ rises with n_{ch}, from 0.8 to 1.2 GeV. This increase is expected due to colour-reconnection effects. The results are compared to various Monte Carlo event generator models. The EPOS LHC [11] and the Pythia 8 [12] tunes describe the data the most accurately. The EPOS reproducing the η, p_{T}, and $\langle p_{\mathrm{T}} \rangle$ distributions best and Pythia 8 A2 describing the multiplicity best in the low and mid-n_{ch} regions.

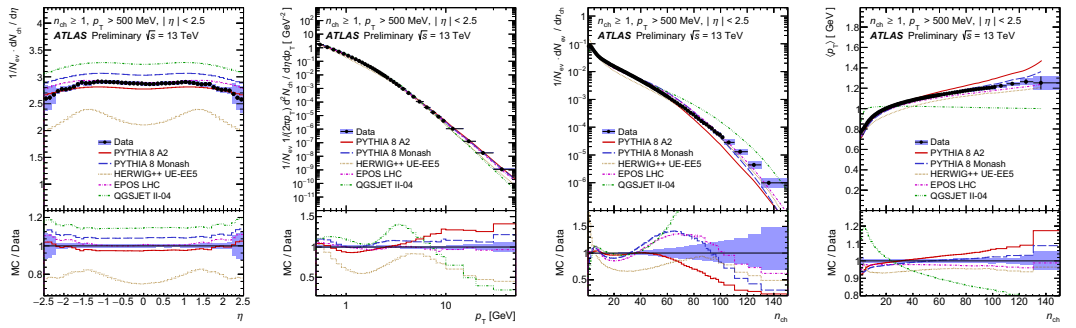

(a) (b) (c) (d)

Figure 2. Charged particle densities as a function of (a) η, (b) p_{T}, (c) n_{ch}, and (d) $\langle p_{\mathrm{T}} \rangle$ dependence on multiplicity. The dots represent the data and the curves the predictions from different MC models. The bottom panels show the ratio of the MC over the data. Taken from Ref. [3].

4 Underlying events at 7 and 13 TeV

A detector level measurement of track distributions sensitive to the properties of the underlying event is given in Ref. [4]. It is based on 9 million events collected using the ATLAS detector in pp collisions at 13 TeV, corresponding to an integrated luminosity of $\approx 170\ \mu\mathrm{b}^{-1}$. The underlying event (UE) is

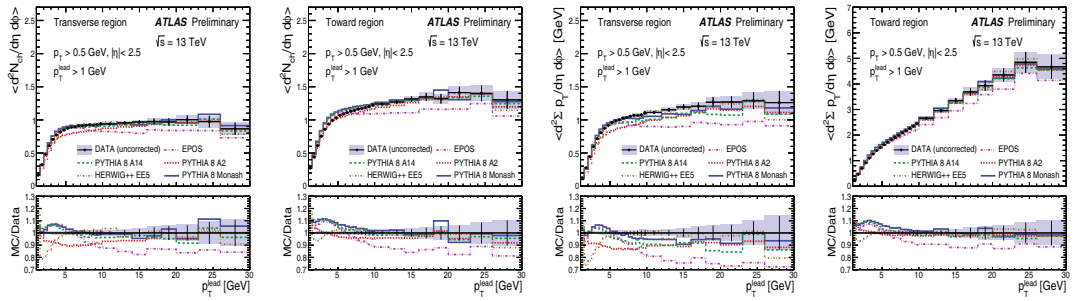

(a) (b) (c) (d)

Figure 3. Comparison of detector level data and MC predictions for (a, b) $\langle d^2 N_{\mathrm{ch}}/d\eta d\phi \rangle$ and (c, d) $\langle d^2 \sum p_{\mathrm{T}}/d\eta d\phi \rangle$ as a function of $p_{\mathrm{T}}^{\mathrm{lead}}$ in the transverse (a, c) and toward (b, d) regions. The bottom panels in each plot show the ratio of MC predictions to data. Taken from Ref. [4].

defined as the activity accompanying any hard scattering in a collision event. This includes partons

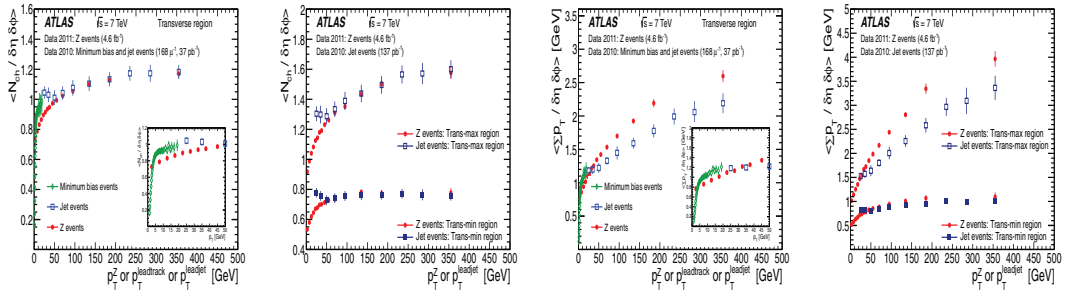

Figure 4. Charged particle multiplicity average values, $N_{\mathrm{ch}}/\delta\eta\delta\phi$ (a, b), and scalar $\sum p_{\mathrm{T}}$ density average values, $\sum p_{\mathrm{T}}/\delta\eta\delta\phi$ (c, d), compared between leading charged particle MB, leading jet and Z-boson events, respectively as functions of leading track $p_{\mathrm{T}}^{\mathrm{lead}}$, leading jet $p_{\mathrm{T}}^{\mathrm{leadjet}}$ and Z-boson p_{T}^{Z}, in the transverse region, trans-max and trans-min-regions, respectively. Taken from Ref. [5].

not participating in the hard-scattering process (beam remnants), and additional scatters in the same pp collision, termed multiple parton interactions (MPI). Initial and final state gluon radiation (ISR, FSR) also contribute to the UE activity. The direction of the leading track is used to define regions in the azimuthal plane that have different sensitivity to the UE. In Fig. 3 the average densities of track multiplicity and scalar $\sum p_{\mathrm{T}}$ are shown. In the transverse region, both show a gradual increase, rising to an approximately constant plateau for $p_{\mathrm{T}}^{\mathrm{lead}} > 6$ GeV. For higher values of $p_{\mathrm{T}}^{\mathrm{lead}}$, the toward and away regions include contributions from jet-like activity, yielding gradually rising average $\sum p_{\mathrm{T}}$ density. Among the MC models, Pythia 8 A14, Monash [12] and Herwig++ [13] predictions are closest to data in the plateau part of the transverse region, but none of the models describe the initial rise well. The EPOS [11] generator predicts significantly less activity at higher $p_{\mathrm{T}}^{\mathrm{lead}}$, indicating the absence of semi-hard MB events.

A measurement of charged particle distributions sensitive to the properties of the underlying event is presented for an inclusive sample of events containing a Z-boson [5] and jets [6]. The measurement is based on data collected using the ATLAS detector in pp collisions at 7 TeV with an integrated luminosity of 4.6 fb^{-1} for Z-boson and 37 pb^{-1} for jets. The certain common qualitative features can be observed by comparing $\sum p_{\mathrm{T}}/\delta\eta\delta\phi$ and $N_{\mathrm{ch}}/\delta\eta\delta\phi$ as functions of the leading object p_{T} in the transverse region, and also separated into the trans-max/min regions as shown in Fig. 4. The measurements with a leading jet are complementary to the measurements with a leading track, and a smooth continuation at 20 GeV is observed (in Fig. 4 (a), (c)), corresponding to the lowest jet p_{T} for which the jet measurement could be performed and the highest leading track momentum included in the leading track analysis. Where the p_{T} of the leading object is less than 50 GeV, a large difference is observed both for the N_{ch} and $\sum p_{\mathrm{T}}$ average values between the jet and Z-boson measurements in Fig. 4 (a), (c); the increase of the associated activity as a function of the hard scale p_{T} is very different in track/jets events from the Z-boson events. The N_{ch} density is similar in the underlying event associated with a jet to that with a Z-boson for higher values of the hard scale ($\geq$ 50 GeV), there are residual differences in the average $\sum p_{\mathrm{T}}$ densities. The activity in events with a Z-boson is systematically higher than that in events with jets. From the behaviour of the underlying event properties in the trans-max/min regions in Fig. 4 (b), (d) this difference originates mostly from the trans-max region, due to selection bias. The trans-min region is very similar between the two measurements, despite the different hard scales, indicating again that this region is least sensitive to the hard interaction and

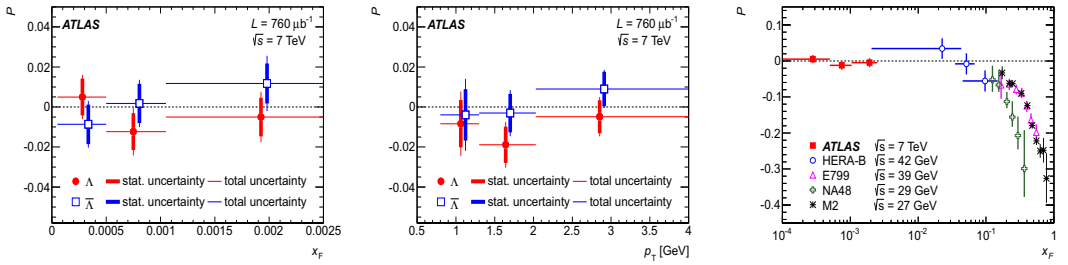

(a) (b) (c)

Figure 5. Transverse polarization of Λ and $\bar{\Lambda}$ hyperons as a function of (a) x_F and (b) p_T (taken from Ref. [7]). The Λ transverse polarization measured by ATLAS compared to the measurements from lower center-of-mass energy experiments HERA-B data taken from Ref. [15], NA48 from Ref. [16], E799 data from Ref. [17], and M2 from Ref. [18].

most sensitive to the MPI component. The measured distributions are compared to the predictions of various Monte Carlo generators implementing different underlying event models.

5 Particleproduction at 7 TeV

The transverse polarization of Λ and $\bar{\Lambda}$ hyperons produced in pp collisions at a center-of-mass energy of 7 TeV is measured in Ref. [7]. The analysis uses 760 μb^{-1} of MB data collected by the ATLAS detector. The measured transverse polarization averaged over Feynman x_F from 5×10^5 to 0.01 and transverse momentum p_T from 0.8 to 15 GeV is 0.010 ± 0.005 $(stat) \pm 0.004$ $(syst)$ for Λ and 0.002 ± 0.006 $(stat) \pm 0.004$ $(syst)$ for $\bar{\Lambda}$. It is also measured as a function of x_F (Fig. 5 (a)) and p_T (Fig. 5 (b)), but no significant dependence on these variables is observed. Prior to this measurement, the polarization was measured at fixed target experiments with center-of-mass energies up to about 40 GeV. The ATLAS results are compatible with the extrapolation of a fit from previous measurements to the x_F range covered by this measurement (Fig. 5 (c)).

A measurement of the $\phi(1020) \times BR(\phi \to K^+K)$ production cross section at 7 TeV is presented using pp collision data corresponding to an integrated luminosity of 383 μb^{-1}, collected with the ATLAS experiment [8]. Selection of $\phi(1020)$-mesons is based on the identification of $K^\pm$ by their energy loss in the pixel detector. The differential cross section is measured as a function of the transverse momentum, $p_{T,\phi}$, (Fig. 6 (a)) and rapidity, y_ϕ, (Fig. 6 (b)) of the $\phi(1020)$-meson in the fiducial region $500 < p_{T,\phi} < 1200$ MeV, $|y_\phi| < 0.8$, kaon $p_{T,K} > 230$ MeV, and kaon momentum $p_K < 800$ MeV. The integrated $\phi(1020)$-meson production cross section in this fiducial range is measured to be $\phi(1020) \times BR(\phi \to K^+K) = 570 \pm 8\,(stat) \pm 66\,(syst) \pm 20\,(lumi)\,\mu$b. The extrapolated cross section is compared to the measurement by the ALICE Collaboration of the $\phi(1020)$ production cross section (see Ref. [19]). A comparison between the cross section measurements is shown in Fig. 6 (c). The measurements as a function of $p_{T,\phi}$ are in agreement to within 10% in the first two bins and to within 3% in the other bins, which is well within the systematic uncertainties. The $\phi(1020)$ production cross section is in agreement with the predictions of the MC generators EPOS [11] and Pythia 6 DW [12].

6 Summary

The Bose-Einstein correlations at 0.9 and 7 TeV were studied. For the first time a saturation effect in the multiplicity dependence of the extracted BEC radius parameter is observed. The k_T dependence

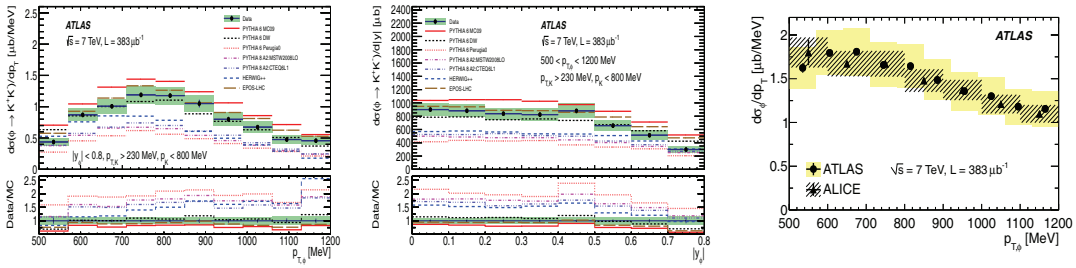

(a) (b) (c)

Figure 6. The $\phi(1020) \times BR(\phi \to K^+K)$ cross section as a function of (a) $p_{\mathrm{T},\phi}$ and (b) $|y_\phi|$ (taken from Ref. [8]). The data are compared to various MC expectations as described in the legends. The $\phi(1020)$-meson cross section as a function of (c) $p_{\mathrm{T},\phi}$ is compared to the measurement by the ALICE Collaboration [19].

on R is observed to increase with multiplicity. Charged particle multiplicity measurements at 13 TeV using pp collisions are presented. Among the models considered, EPOS reproduces the data the best way, Pythia 8 A2 and Monash give reasonable descriptions. Underlying event analysis with 13 TeV data are shown: one observes a reasonable agreement of tunes used in Atlas MC with the new data. Further UE studies were done at 7 TeV for Z, leading jet and leading track. These are required for tuning of the soft part of Monte Carlo simulation. Transverse polarisation of Λ and $\bar{\Lambda}$ hyperons at 7 TeV were found to be consistent with 0 at low x_{F}, confirming the behaviour of previous experiments showing a decrease of polarization as function of x_{F}. The measurement of $\phi(1020)$ differential cross section at 7 TeV can provide useful input for turning and development of phenomenological models.

References

[1] ATLAS Collaboration, JINST **3** S08003 (2008)
[2] ATLAS Collaboration, Eur. Phys. J. C **75**, 10, 466 (2015) [arXiv:1502.07947]
[3] ATLAS Collaboration, ATLAS-CONF-2015-028, https://cds.cern.ch/record/2037701
[4] ATLAS Collaboration, ATL-PHYS-PUB-2015-019, https://cds.cern.ch/record/2037684
[5] ATLAS Collaboration, Eur. Phys. J. C **74**, 12, 3195 (2014) [arXiv:1409.3433]
[6] ATLAS Collaboration, Eur. Phys. J. C **74**, 8, 2965 (2014) [arXiv:1406.0392]
[7] ATLAS Collaboration, Phys. Rev. D **91**, 3, 032004 (2015) [arXiv:1412.1692]
[8] ATLAS Collaboration, Eur. Phys. J. C **74**, 7, 2895 (2014) [arXiv:1402.6162]
[9] T. Alexopoulos *et al.*, Phys. Rev. D **48**, 1931 (1993)
[10] M.M. Aggarwal *et al.*, STAR Collaboration, Phys. Rev. C **83**, 064905 (2011)
[11] S. Porteboeuf, T. Pierog and K. Werner [arXiv:1006.2967]
[12] T. Sjöstrand, S. Mrenna and P. Z. Skands, Comput. Phys. Commun. **178**, 852867 (2008)
[13] M. Bahr *et al.*, Eur. Phys. J. C **58** 639707 (2008)
[14] S. Ostapchenko, Phys. Rev. D **83** 014018 (2011)
[15] I. Abt *et al.*, HERA-B Collaboration, Phys. Lett. B **638**, 415 (2006)
[16] V. Fanti *et al.*, NA48 Collaboration, Eur. Phys. J. C **6**, 265 (1999)
[17] E. Ramberg *et al.*, E799 Collaboration, Phys. Lett. B **338**, 403 (1994)
[18] B. Lundberg *et al.*, Phys. Rev. D **40**, 3557 (1989)
[19] ALICE Collaboration, Eur. Phys. J. C **72**, 2183 (2012)